



Communication

Structural, electronic, mechanical, dielectric and optical properties of TiSiO₄: First-principles studyHao Liu^{a,b,c}, Zheng-Tang Liu^d, Juan Ren^e, Qi-Jun Liu^{a,b,*}^a School of Physical Science and Technology, Southwest Jiaotong University, Key Laboratory of Advanced Technologies of Materials, Ministry of Education of China, Chengdu 610031, People's Republic of China^b Bond and Band Engineering Group, Sichuan Provincial Key Laboratory (for Universities) of High Pressure Science and Technology, Southwest Jiaotong University, Chengdu 610031, People's Republic of China^c School of Information Science and Technology, Fudan University, Shanghai 200433, People's Republic of China^d State Key Laboratory of Solidification Processing, Northwestern Polytechnical University, Xi'an 710072, People's Republic of China^e School of Science, Xi'an Technological University, Xi'an 710032, People's Republic of China

ARTICLE INFO

Keywords:

A: TiSiO₄

D: Elastic properties

D: Electronic properties

E: First-principles calculations

ABSTRACT

Using the first-principles calculations, we have computed the structural parameters, band structures, elastic, dielectric and optical properties of TiSiO₄ in orthorhombic CrVO₄-type (*Cmcm*), tetragonal zircon-type (*I4₁/amd*) and scheelite-type (*I4₁/a*) phases. The obtained structural parameters of three phases were in agreement with previous results. The band structures, density of states and bond populations have been given to analyze the electronic properties and chemical bondings. The independent elastic constants of three phases have been calculated, showing that all of them were mechanically stable. The CrVO₄ phase showed a brittle manner and the others behaved in a ductile manner. Moreover, the permittivity, refractive index, extinction coefficient, reflectivity, absorption coefficient, loss function and optical conductivity of three phases have been obtained and analyzed.

1. Introduction

In semiconductor industry, the downscaling of feature size in metal-oxide-semiconductor field effect transistor (MOSFET) results in many problems. The most crucial problem affecting properties of transistors is the leakage current through the thin gate oxide layer [1,2]. One effective method reducing leakage current is replacement of the traditional transistors [3], but there is still a long way for theoretical and experimental studies. Another useful and feasible method is to replace the common SiO₂ gate oxide by new high-κ materials [1,2]. There are extensive studies on potential high-κ materials, e.g. transition metal oxides (TMOs) [4–6]. Many of them have promising electronic properties, such as HfO₂, TiO₂ and ZrO₂. However, high dielectric constant is one of the basic characteristics for alternative gate oxides to replace SiO₂. They must have thermodynamic stability on Si substrates, good electrical interface properties, few bulk electrically active defects, and large band offsets with Si [1]. Compared with SiO₂ deposited on Si substrates, transition metal oxides usually have bad interface properties with Si substrates [7]. Hence, transition metal silicates with high permittivity and good interface properties attract our attention, which are potential candidates for gate oxides [4].

Most recently, three possible structures of TiSiO₄ have been predicted, and their structural characteristics and phonon frequencies at the *Γ* point also have been detailedly studied by DFT calculations [8]. TiSiO₄ ceramics have been prepared via the sol-gel process and their thermodynamic stability and permittivity were investigated [9], indicating that TiSiO₄ was thermodynamic stability and could be used as high-κ materials.

In this paper, we study band structures, density of states, elastic properties and dielectric tensors of three predicted structures of TiSiO₄ by first-principles calculations. The rest of this paper is organized as follow: the computational details are shown in Section 2, the calculated data and analysis of TiSiO₄ are given in Section 3, and the conclusions are presented in Section 4.

2. Computational details

The periodic DFT calculations [10] were performed using the plane-wave ultrasoft pseudopotential method with the generalized gradient approximation (GGA) with Perdew-Wang (PW91) functional implemented in the CASTEP code. The plane-wave cutoff energy of 380eV has been used. The valence electron configurations for O, Si and Ti

* Corresponding author at: School of Physical Science and Technology, Southwest Jiaotong University, Chengdu, Sichuan 610031, People's Republic of China.
E-mail address: qijunliu@home.swjtu.edu.cn (Q.-J. Liu).

<http://dx.doi.org/10.1016/j.ssc.2016.12.013>

Received 30 August 2016; Received in revised form 13 December 2016; Accepted 19 December 2016

Available online 21 December 2016

0038-1098/ © 2016 Elsevier Ltd. All rights reserved.

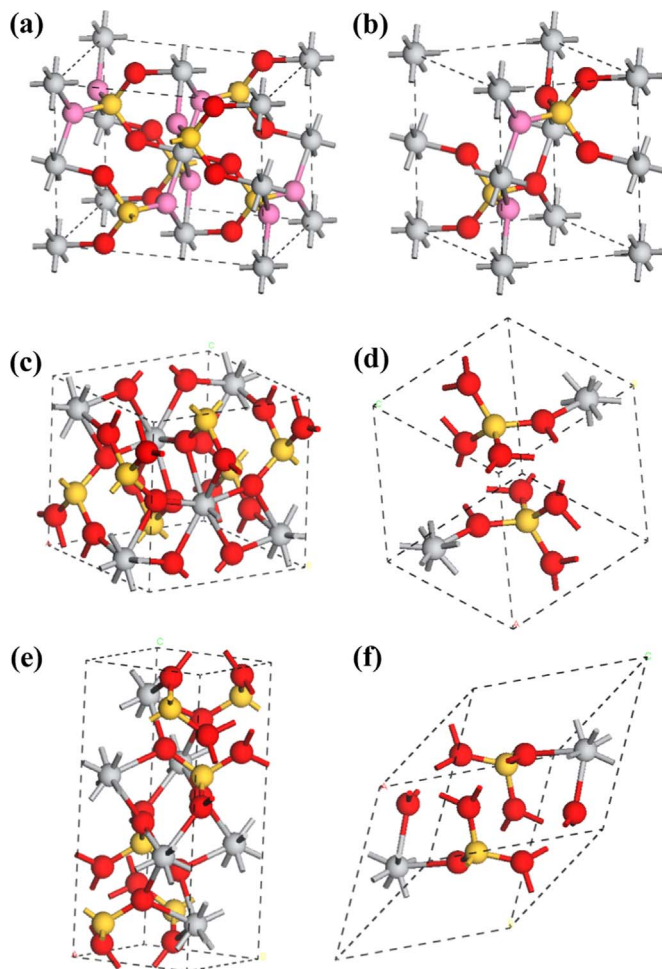


Fig. 1. Structures of TiSiO_4 : (a) and (b) CrVO_4 phase, (c) and (d) zircon phase, (e) and (f) scheelite phase (a, c and e: conventional cell, b, d and f: primitive cell. Ti, Si and O atoms are in gray, yellow and red (O2 atoms in CrVO_4 phase are in pink)).

atoms were $02s^22p^4$, $\text{Si}3s^23p^2$ and $\text{Ti}3s^23p^63d^24s^2$. The convergence thresholds for total energy, maximum force, maximum stress, and maximum displacement were less than $5 \times 10^{-6} \text{eV/atom}$, 0.01eV/\AA , 0.02GPa and $5.0 \times 10^{-4} \text{\AA}$, respectively. It is well-known that the DFT-GGA calculations underestimate bandgaps [11]. We here used the hybrid functional calculations with PBE0 functional to solve this problem. Moreover, the density functional perturbation theory (DFPT) has been used to calculate the dielectric properties of TiSiO_4 .

3. Results and analysis

3.1. Structural properties

The CrVO_4 -type, zircon-type and scheelite-type TiSiO_4 belong to $Cmcm$, $I4_1/amd$, and $I4_1/a$ space group [8], which are shown in Fig. 1. The Ti, Si, O1 and O2 atoms of CrVO_4 -type phase occupy at $(0,0,0)$, $(0,0.3470,0.25)$, $(0,0.2284,0.0414)$ and $(0.2527,0.4707,0.25)$ [8], respectively. The Ti, Si and O atoms of zircon-type phase are at $(0,0.75,0.125)$, $(0,0.25,0.375)$ and $(0,0.0578,0.1918)$ [8]. The Ti, Si and O atoms of scheelite-type phase are at $(0,0.25,0.625)$, $(0,0.25,0.125)$ and $(0.2651,0.0719,0.0471)$ [8]. After geometry optimization, the optimized lattice parameters of three phases are listed in Table 1, together with the available theoretical data [8,12]. It can be seen that the cell volumes per formula unit of CrVO_4 -type, Zircon-type and Scheelite-type TiSiO_4 are 67.58 \AA^3 , 59.21 \AA^3 and 54.36 \AA^3 , respectively. They are slightly larger than the reported values [8], with 1.93%, 1.91% and 3.54%. Overall, our calculated results of three phases are reasonable.

3.2. Electronic properties

TiSiO_4 is a potential grid electrode material in metal-oxide-semiconductor effect transistors, so its bandgap is a vital characterization to judge whether it can replace SiO_2 . The band structures of three phases of TiSiO_4 are shown in Fig. 2 (Fermi energy is set as 0 eV). We can see that three different phases of TiSiO_4 all have an indirect bandgap. For CrVO_4 -type, the maximum of valence bands and the minimum of conduction bands are at $\Gamma(G)$ and Y , respectively. The calculated value of the bandgap is 1.750 eV. The bandgap of zircon-type is the largest

Table 1
Calculated structural parameters and atomic positions of TiSiO_4 .

	CrVO_4	Zircon	Scheelite	
$a(\text{\AA})$	5.3458	6.3206	4.5850	
	5.2957	6.2570	4.5536	[8] [12]
$b(\text{\AA})$	8.0531	6.3206	4.5850	
	7.9996	6.2570	4.5536	[8] [12]
$c(\text{\AA})$	6.2792	5.9289	10.3440	
	6.2554	5.9351	10.1277	[8] [12]
$V(\text{\AA}^3)$	67.58	58.1	54.36	
	66.3	56.02	52.5	[8] [12]
$\rho(\text{g/cm}^3)$	3.4396	3.9255	4.2757	
Ti(x, y, z)	(0,0,0)	(0,0.75,0.125)	(0,0.25,0.625)	
Si(x, y, z)	(0,0,0)	(0,0.75,0.125)	(0,0.25,0.625)	[8]
	(0,0.3477,0.25)	(0,0.25,0.375)	(0,0.25,0.125)	
	(0,0.3470,0.25)	(0,0.25,0.375)	(0,0.25,0.125)	[8]
O ₁ (x, y, z)	(0,0.2283,0.0441)	(0,0.0589,0.1918)	(0.2650,0.0713,0.0497)	
	(0,0.2284,0.0414)	(0,0.0578,0.1918)	(0.2651,0.0719,0.0471)	[8] [12]
O ₂ (x, y, z)	(0.2518,0.4690,0.25)	(0,0.0591,0.1892)		[8]
	(0.2527,0.4707,0.25)			

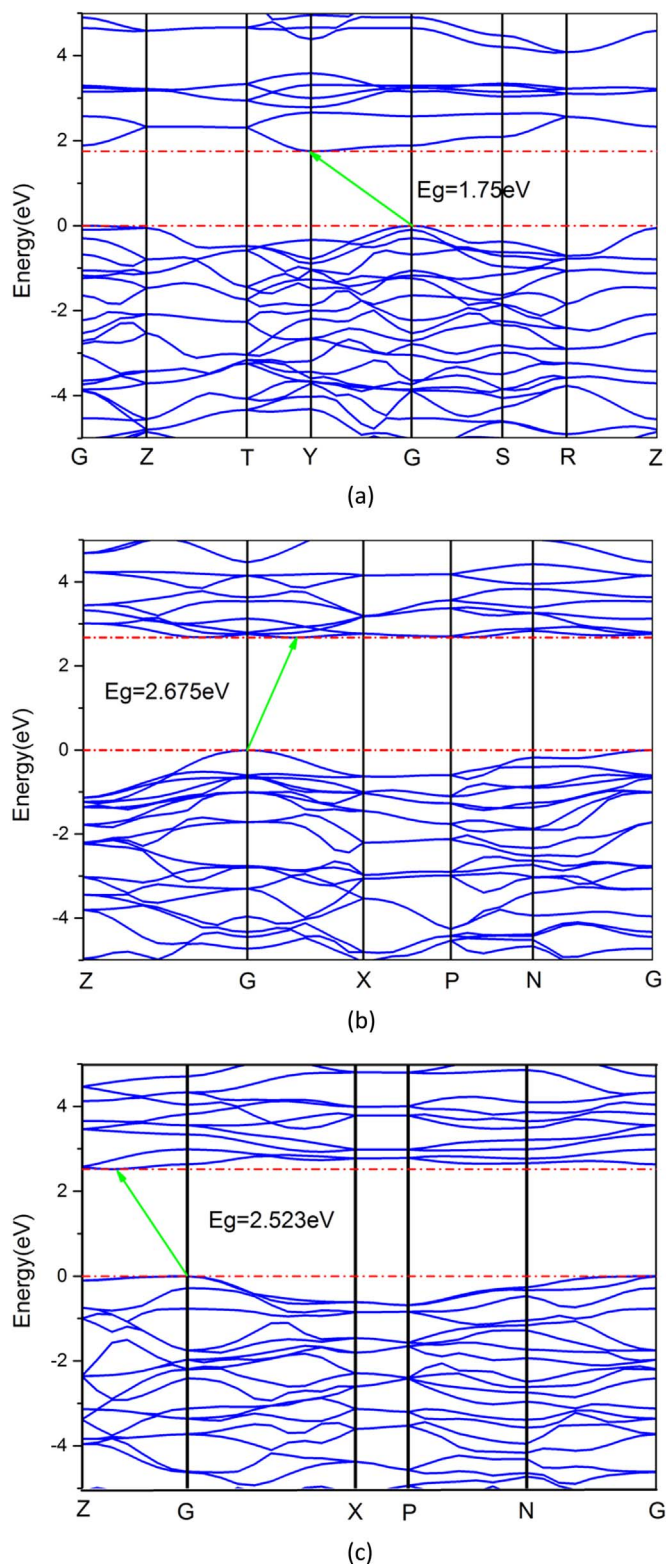


Fig. 2. Band structures of TiSiO_4 (a) CrVO_4 -type, (b) Zircon-type, (c) Scheelite-type.

bandgap in three phases, whose value is calculated to be 2.675eV. The bandgap value of scheelite-type is larger than that of $Cmcm$ phase, which is 2.523eV. Compared with the previous values [8] (the B3LYP calculations), our results are smaller due to the underestimation of GGA calculations [11]. Hence, we apply the PBE0 functional to calculate the bandgap of TiSiO_4 . The calculated results are given in Table 2. It's obvious that the results of PBE0 calculations are larger

Table 2
Calculated bandgaps (eV) along with the available data [8].

	CrVO_4	Zircon	Scheelite
GGA	1.750	2.675	2.523
B3LYP[8]	3.49	4.50	4.27
PBE0	4.390	5.302	5.101

than those of GGA calculations. The change trend of bandgap values is consistent with the reported results [8].

We calculate the total and partial density of states of three structures of TiSiO_4 for further analysis, which are shown in Fig. 3. Combining the band structures with density of states of three phases of TiSiO_4 , we find that the upper valence bands are mainly due to O-2p states with some mixings of Ti-3d and Si-3p states. The lower conduction bands are mainly contributed by Ti-3d states with some mixings of O-2p states. Then, we investigate the bond populations of TiSiO_4 to analyze the chemical bonding. We calculate both bond populations and bond lengths, which are shown in Table 3. We analyze the bond populations together with the structural characteristics. The bonding and antibonding states are associated with the positive and negative values of populations, and a high value of population shows a high degree of covalent nature for bonds [13]. For CrVO_4 -type, the Ti-O bonds in TiO_6 octahedron can be separated into two groups, namely O1-Ti and O2-Ti. The length of O1-Ti bonds is shorter than that of O2-Ti bonds. The covalent nature of O1-Ti bonds is larger than that of O2-Ti bonds due to the bigger bond population. The Si-O bonds in SiO_4 tetrahedron have two different types of Si-O bonds, namely O1-Si and O2-Si. The covalent nature of O1-Si is larger than that of O2-Si. For two tetragonal phases, the Si-O bonds in SiO_4 tetrahedron and the Ti-O bonds in TiO_8 dodecahedron show covalent nature. The calculated bond populations of Si-O bonds and Ti-O bonds are 0.59 and 0.37, 0.57 and 0.32 in zircon-type and scheelite-type, respectively. Hence, the degree of covalent nature in zircon-type is larger than that in scheelite-type.

3.3. Elastic constants, mechanical properties and sound velocity

Elastic constants are important for us to estimate material's mechanical stability. We can obtain mechanical modulus and sound velocity from these parameters. The calculated independent elastic stiffness constants C_{ij} are presented in Table 4. The obtained independent elastic stiffness constants indicate that the chemical bonds along the [100] direction are stronger than those along others two directions, because C_{11} is much larger than C_{22} and C_{33} . For tetragonal zircon-type phase, the elastic constants C_{11} , C_{22} and C_{33} are nearly the same. The chemical bonds along the [100] and [010] directions are larger than those along the [001] direction for scheelite phase.

We estimate the mechanical stability for three structures of TiSiO_4 by Born stability criteria. For orthorhombic phase, the stability criteria are given by [14]:

$$\begin{aligned}
 &C_{11} > 0, C_{22} > 0, C_{33} > 0, C_{44} > 0, C_{55} > 0, C_{66} \\
 &> 0, [C_{11} + C_{22} + C_{33} + 2(C_{12} + C_{13} + C_{23})] > 0, (C_{11} + C_{22} - 2C_{12}) \\
 &> 0, (C_{11} + C_{33} - 2C_{13}) > 0, (C_{22} + C_{33} - 2C_{23}) > 0
 \end{aligned} \quad (1)$$

For tetragonal phase, the mechanical stability criteria are [14]:

$$\begin{aligned}
 &C_{11} > 0, C_{33} > 0, C_{44} > 0, C_{66} > 0, (C_{11} - C_{12}) > 0, (C_{11} + C_{33} - 2C_{13}) \\
 &> 0, [2(C_{11} + C_{12}) + C_{33} + 4C_{13}] > 0
 \end{aligned} \quad (2)$$

These criteria are satisfied for all structures of TiSiO_4 , indicating that three phases are mechanical stability. Besides the mechanical stability, the energetic and dynamical stability should be further discussed. The relatively calculated results of structural stability and phonon frequencies have been shown [8,12,15].

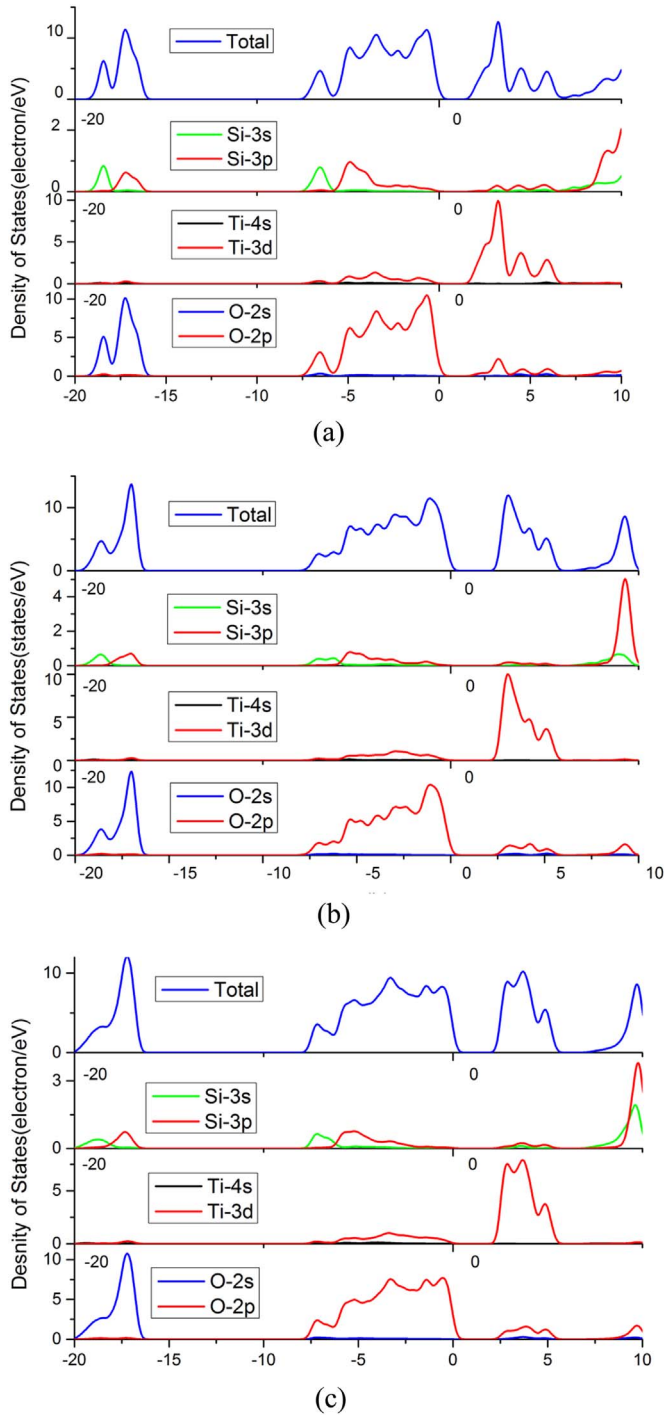


Fig. 3. Total and partial density of states of TiSiO_4 (a) CrVO_4 -type, (b) Zircon-type, (c) Scheelite-type.

Table 3
Calculated bond populations and bond lengths (Å) of three different phases of TiSiO_4 .

	CrVO_4		Zircon		Scheelite	
	Bond population	Length	Bond population	Length	Bond population	Length
O1–Si	0.65	1.6112	0.59	1.6246	0.57	1.6599
O2–Si	0.52	1.6630				
O1–Ti	0.49	1.8592	0.37	1.9921	0.32	1.9845
O2–Ti	0.28	2.0706				

According to the Voigt-Reuss-Hill [16–18] approximation (The Voigt and Reuss approximations represent the equality of uniform strain to external stress and the equality of uniform stress to external stress, respectively. The Hill approximation applies the arithmetic average of the above two methods), we calculate bulk modulus B , shear modulus G , Young's modulus E , compressibility β , Poisson's ratio ν , Lamé's constants μ and λ , which are shown in Table 5. It can be seen that our calculated bulk modulus of CrVO_4 -type phase is 120.03 GPa that is excellent agreement with previous theoretical value of 124.0 GPa [8]. For Zircon-type phase, the previous theoretical value of bulk modulus is 248.4 GPa [8], which is larger than our value of 222.26 GPa. For scheelite-type phase, we notice that our calculated value has the discrepancy of 17.83 % compared to previous theoretical value (238.2 GPa [8]). We conclude that zircon-type phase has largest bulk modulus and lowest compressibility. The B/G ratio has been extensively used to judge the ductility of materials [19]. We calculate the ratios of CrVO_4 -type, zircon-type and scheelite-type phases, which are 1.484, 2.177 and 2.747, respectively. The critical value to identify ductile or brittle materials is 1.75, so we can see that CrVO_4 -type phase is brittle and the others phases are ductile.

According to the obtained mechanical modulus, the shear sound velocity v_s , compressional sound velocity v_p and average sound velocity v_m can be calculated by following formulas [20]:

$$v_s = \sqrt{\frac{G_X}{\rho}} \quad (3)$$

$$v_p = \sqrt{\frac{B_X + \frac{4G_X}{3}}{\rho}} \quad (4)$$

$$v_m = \left[\frac{(2/v_s^3 + 1/v_p^3)}{3} \right]^{-1/3} \quad (5)$$

It is well-known that the stronger hybridization between optical and acoustic phonon modes is, the smaller thermal conductivity is $k \sim v^3$ [21]. The relationship between thermal conductivity and sound velocity is $k \sim v^3$ [21]. It can be seen that zircon-type and scheelite-type have the largest and lowest sound velocity (Table 6), respectively, meaning that the order of thermal conductivity is zircon > CrVO_4 > scheelite. The lowest thermal conductivity of scheelite-type phase indicates the relatively strong hybridization between optical and acoustic phonon modes.

3.4. Dielectric properties

The large permittivity of TiSiO_4 is important to its application as alternative high- κ material. The permittivity of a crystal can be described as static dielectric tensor ϵ_0 that can be decomposed into two components. One is electronic contribution ϵ_∞ and the other is lattice contribution $\epsilon_{\text{lattice}}$, namely $\epsilon_0 = \epsilon_\infty + \epsilon_{\text{lattice}}$. The lattice contribution $\epsilon_{\text{lattice}}$ is obtained by IR-active phonon modes, which is calculated by following formula [22]:

$$\epsilon_{\alpha\beta}^{\text{lattice}} = \frac{4\pi e^2}{M_0 \Omega} \sum_{\lambda} \frac{\tilde{Z}_{\lambda\alpha}^* \tilde{Z}_{\lambda\beta}}{\omega_{\lambda}^2} \quad (6)$$

where the $\tilde{Z}_{\lambda\alpha}^* = \sum_{i\beta} Z_{i,\alpha\beta}^* (M_0/M_i)^{1/2} \xi_{i,\lambda\beta}$ are the mode effective charges, $Z_{i,\alpha\beta}^*$ is the Born effective charge tensor for ion i , M_i is its mass, e is the electron charge, M_0 is the reference mass that is set as 1 amu, ω_{λ} is the frequency of λ th infrared-active phonon mode, Ω is the volume of unit cell. $\xi_{i,\lambda\beta}$ is the eigendisplacement of atom i in phonon mode λ , which is normalized according to

$$\sum_{i\alpha} \xi_{i,\lambda\alpha} \xi_{i,\lambda,\beta} = \delta_{\lambda\lambda}^i \quad (7)$$

Due to the orthogonal symmetry of CrVO_4 phase, its ϵ_∞ and $\epsilon_{\text{lattice}}$ dielectric tensors have three independent components ϵ_{xx} , ϵ_{yy} and ϵ_{zz} .

Table 4
Calculated independent elastic stiffness constants C_{ij} (GPa) for TiSiO_4 .

	C_{11}	C_{22}	C_{33}	C_{12}	C_{13}	C_{23}	C_{44}	C_{55}	C_{66}	C_{16}
CrVO ₄	300.65	190.27	205.53	98.54	62.80	48.03	112.56	67.39	73.23	
Zircon	380.22		390.77	88.08	172.23		107.19		71.23	
Scheelite	461.34		195.14	189.26	116.26		38.77		98.82	-6.53

Table 5
Calculated values of bulk modulus B (GPa), shear modulus G (GPa), Young's modulus E (GPa), compressibility β (GPa^{-1}), Poisson's ratio ν , Lamé's constants μ and λ (GPa).

	B_X			G_X (μ_X)			E_X		
	$X=R$	$X=V$	$X=H$	$X=R$	$X=V$	$X=H$	$X=R$	$X=V$	$X=H$
CrVO ₄	116.14	123.91	120.03	78.69	83.11	80.90	192.58	203.77	198.18
Zircon	220.48	224.03	222.26	99.18	105.03	102.11	258.74	272.50	265.65
Scheelite	173.53	217.93	195.73	60.83	81.67	71.25	163.40	217.80	190.62
	ν_X			$\beta_X (\times 10^{-3})$			λ_X		
	$X=R$	$X=V$	$X=H$	$X=R$	$X=V$	$X=H$	$X=R$	$X=V$	$X=H$
CrVO ₄	0.2236	0.2259	0.2248	8.61	8.07	8.33	63.68	68.50	66.10
Zircon	0.3044	0.2973	0.3008	4.54	4.46	4.50	154.36	154.01	154.19
Scheelite	0.3431	0.3334	0.3377	5.76	4.59	5.11	132.98	163.48	148.23

Table 6
Shear, compressional and average sound velocities of TiSiO_4 .

	v_s^X (m/s)			v_p^X (m/s)			v_m^X (m/s)		
	$X=R$	$X=V$	$X=H$	$X=R$	$X=V$	$X=H$	$X=R$	$X=V$	$X=H$
CrVO ₄	4783	4916	4850	8017	8261	8140	5294	5442	5369
Zircon	5026	5173	5100	9479	9630	9555	5618	5776	5697
Scheelite	3772	4370	4082	7717	8743	8246	4237	4903	4582

While zircon phase and scheelite phase are tetragonal symmetry, their dielectric tensors have two independent components ϵ_{\parallel} and ϵ_{\perp} , parallel and perpendicular to the c axis, respectively. The calculated values of ϵ_{∞} and ϵ_0 dielectric tensors are as follows:

$$\epsilon_{\infty}^{cmcm} = \begin{bmatrix} 3.92 & 0 & 0 \\ 0 & 4.91 & 0 \\ 0 & 0 & 4.46 \end{bmatrix}$$

$$\epsilon_{\infty}^{zircon} = \begin{bmatrix} 5.52 & 0 & 0 \\ 0 & 5.52 & 0 \\ 0 & 0 & 5.43 \end{bmatrix}$$

$$\epsilon_{\infty}^{scheelit} = \begin{bmatrix} 5.95 & 0 & 0 \\ 0 & 5.95 & 0 \\ 0 & 0 & 5.73 \end{bmatrix}$$

$$\epsilon_0^{cmcm} = \begin{bmatrix} 13.04 & 0 & 0 \\ 0 & 15.81 & 0 \\ 0 & 0 & 10.81 \end{bmatrix}$$

$$\epsilon_0^{zircon} = \begin{bmatrix} 27.09 & 0 & 0 \\ 0 & 27.09 & 0 \\ 0 & 0 & 19.37 \end{bmatrix}$$

$$\epsilon_0^{scheelite} = \begin{bmatrix} 21.27 & 0 & 0 \\ 0 & 21.27 & 0 \\ 0 & 0 & 16.85 \end{bmatrix}$$

It is important to note that three phases of TiSiO_4 have a similar electronic dielectric constant ϵ_{∞} ($\approx 5 \pm 1$). The main contribution of static dielectric constant comes from lattice dielectric constant. Table 7 shows the calculated electronic $\epsilon_{\infty} = (\epsilon_{\infty}^x + \epsilon_{\infty}^y + \epsilon_{\infty}^z)/3$ and static $\epsilon_0 = (\epsilon_0^x + \epsilon_0^y + \epsilon_0^z)/3$ dielectric constants for CrVO₄ phase, zircon phase

Table 7
Calculated electronic ϵ_{∞} and static ϵ_0 dielectric constants for CrVO₄ phase, Zircon phase and Scheelite phase of TiSiO_4 .

	CrVO ₄	Zircon	Scheelite
ϵ_{∞}	4.43	5.49	5.88
ϵ_{∞} [8]	3.59	4.46	4.78
ϵ_{∞} [12]		5.55	
ϵ_0	13.22	24.52	19.80
ϵ_0 [12]		18.54	

and scheelite phase of TiSiO_4 . Compared with available theoretical data [8], we find that our calculated electronic dielectric constants ϵ_{∞} are lightly bigger. The value of 5.49 for zircon phase is close to the previous value of 5.55 [12]. The zircon phase has largest static dielectric constant, and the lattice dielectric constant of zircon phase is bigger than that of the others phases. Recently, the TiSiO_4 ceramics have been obtained via sol-gel method [9]. The authors found that TiSiO_4 ceramics were thermal stability in the range of -20 to 75°C and the average relative permittivity was $\epsilon_r = 17.75$. It can be seen that our calculated results are consistent with experimental data.

3.5. Optical properties

The frequency-dependent dielectric function $\epsilon(\omega) = \epsilon_1(\omega) + i\epsilon_2(\omega)$ determines the optical properties of materials. We can acquire refractive index $n(\omega)$, extinction coefficient $k(\omega)$, reflectivity $R(\omega)$, absorption coefficient $I(\omega)$, loss function $L(\omega)$ and optical conductivity $\sigma(\omega)$ as follows [23,24]:

$$n(\omega) = \left[\frac{\epsilon_1(\omega) + \sqrt{\epsilon_1(\omega)^2 + \epsilon_2(\omega)^2}}{2} \right]^{1/2} \tag{8}$$

$$k(\omega) = \left[\frac{\sqrt{\epsilon_1(\omega)^2 + \epsilon_2(\omega)^2} - \epsilon_1(\omega)}{2} \right]^{1/2} \tag{9}$$

$$R(\omega) = \left[\frac{\frac{1}{\epsilon^2}(\omega) - 1}{\frac{1}{\epsilon^2}(\omega) + 1} \right]^2 \tag{10}$$

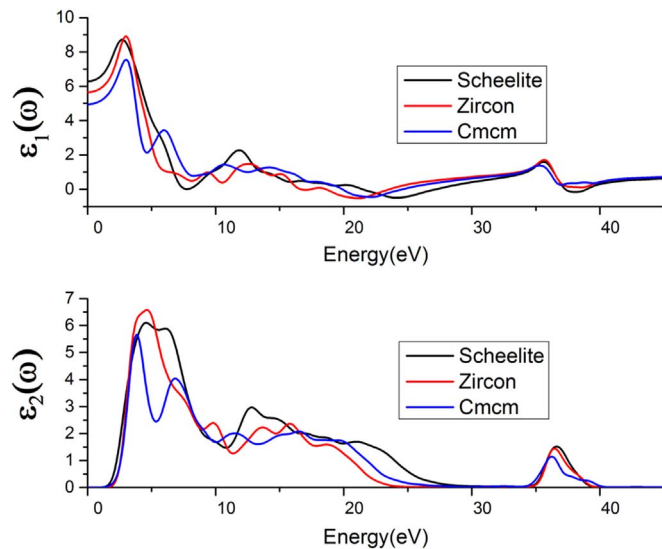


Fig. 4. Real and imaginary parts of complex dielectric function for TiSiO_4 .

$$I(\omega) = \sqrt{2} (\sqrt{\varepsilon_1(\omega)^2 + \varepsilon_2(\omega)^2} - \varepsilon_1(\omega))^{1/2} \quad (11)$$

$$L(\omega) = \frac{\varepsilon_2(\omega)}{\varepsilon_1(\omega)^2 + \varepsilon_2(\omega)^2} \quad (12)$$

$$\sigma(\omega) = \sigma_1(\omega) + \sigma_2(\omega) = -\frac{i\omega}{4\pi} [\varepsilon(\omega) - 1] \quad (13)$$

The calculated dielectric function and optical properties for three phases of TiSiO_4 are shown in Figs. 4 and 5. At low frequency, the refractive index equals the square root of dielectric function. Our results are consistent with above conclusion, which indicates the reasonability of our calculations. The absorption coefficient is associated with $\varepsilon_2(\omega)$, so its curves of TiSiO_4 start in accordance with the optical band gap in $\varepsilon_2(\omega)$. The peaks of loss function $L(\omega)$ are associated with the frequency of plasma resonance. There are two transition points in TiSiO_4 : the first point located at 24.85 eV, 23.63 eV and 27.45 eV, the second point located at 37.25 eV, 38.88 eV and 39.06 eV for CrVO_4 type, zircon type and scheelite type phases, which also correspond to the abrupt decrease of reflectivity curves. The complex conductivity function shows the material's response to a time-varying external electrical field of frequency. We hope our work can help to future research.

4. Conclusions

Three different crystal structures of TiSiO_4 were studied by using first-principles calculations based on DFT. The lattice parameters, band structures, elastic constants, permittivity and optical properties are obtained. Our calculated lattice parameters are in agreement with previous theoretical data. Both GGA and PBE0 calculations show that the zircon phase has largest bandgap. Elastic constants reveal that three structures of TiSiO_4 are mechanically stable. Zircon phase has largest bulk, shear and young's modulus of 222.26 GPa, 102.11 GPa and 265.65 GPa, respectively. We find that CrVO_4 phase behaves in a brittle manner while the others phases show ductile manner. As for permittivity, zircon phase having largest static dielectric constant results from highest lattice dielectric constant, whose static dielectric constant is about 24.52.

Acknowledgments

This work was supported by the National Natural Science Foundation of China (Grant nos. 51402244 and 11547152), the

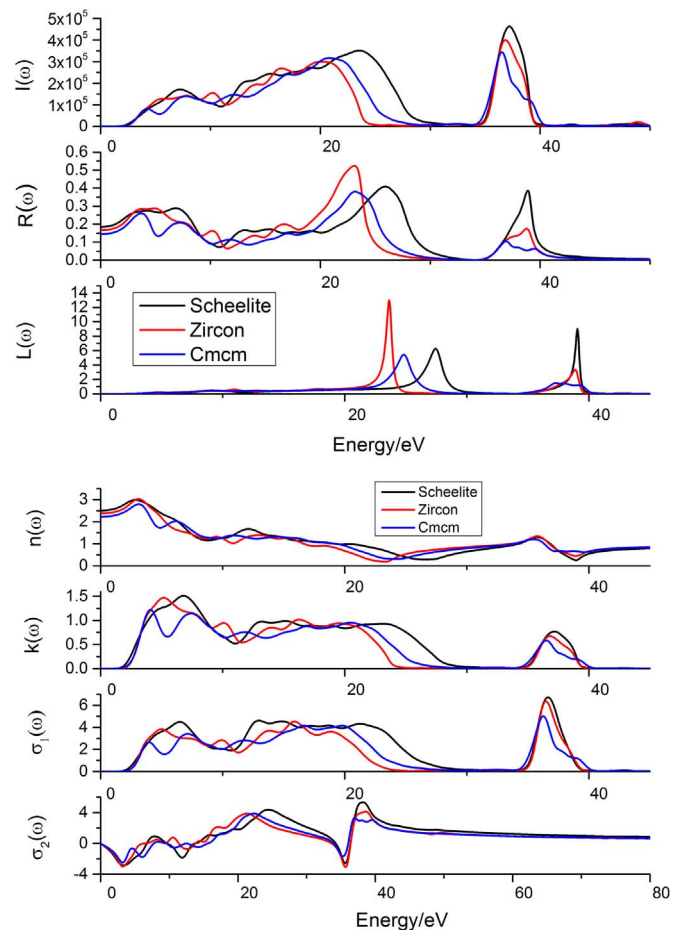


Fig. 5. The calculated optical properties (refractive index $n(\omega)$, extinction coefficient $k(\omega)$, reflectivity $R(\omega)$, absorption coefficient $I(\omega)$, loss function $L(\omega)$ and optical conductivity $\sigma(\omega)$) of TiSiO_4 .

Fundamental Research Fund for the Central Universities, China (Grant no. 2682014ZT31), the fund of the State Key Laboratory of Solidification Processing in NWP (Grant no. SKLSP201511).

References

- [1] J. Robertson, High dielectric constant gate oxides for metal oxide Si transistors, Rep. Prog. Phys. 69 (2006) 327–396.
- [2] K. Cho, First-principles modeling of high-k gate dielectric materials, Comput. Mater. Sci. 23 (2002) 43–47.
- [3] R. Jansen, The spin-valve transistor: a review and outlook, J. Phys. D: Appl. Phys. 36 (2003) R289–R308.
- [4] G.M. Rignanese, Dielectric properties of crystalline and amorphous transition metal oxides and silicates as potential high- κ candidates: the contribution of density-functional theory, J. Phys.: Condens. Matter 17 (2005) R357–R379.
- [5] X. Zhao, D. Vanderbilt, First-principles study of structural, vibrational, and lattice dielectric properties of hafnium oxide, Phys. Rev. B 65 (2002) 233106.
- [6] Q.J. Liu, N.C. Zhang, F.S. Liu, Z.T. Liu, Structural, electronic, optical, elastic properties and Born effective charges of monoclinic HfO_2 from first-principles calculations, Chin. Phys. B 23 (2014) 047101.
- [7] S. Stemmer, Thermodynamic considerations in the stability of binary oxides for alternative gate dielectrics in complementary metal–oxide–semiconductors, J. Vac. Sci. Technol. B 22 (2004) 791–800.
- [8] L. Gracia, A. Beltrán, D. Errandonea, Characterization of the TiSiO_4 structure and its pressure-induced phase transformations: density functional theory study, Phys. Rev. B 80 (2009) 094105.
- [9] J. Varghese, T. Joseph, M.T. Sebastian, Sol-gel derived TiSiO_4 ceramics for high-k gate dielectric applications, AIP Conference Proceedings 1372193–197, 2011.
- [10] (a) S.J. Clark, M.D. Segall, C.J. Pickard, P.J. Hasnip, M.J. Probert, K. Refson, M.C. Payne, First principles methods using CASTEP, Z. Krist. 220 (2005) 567–570
(b) J.P. Perdew, J.A. Chevary, S.H. Vosko, K.A. Jackson, M.R. Pederson, D.J. Singh, C. Fiolhais, Atoms, molecules, solids, and surfaces: applications of the generalized gradient approximation for exchange and correlation, Phys. Rev. B 46 (1992) 6671.

- [11] (a) F. Tran, P. Blaha, Accurate band gaps of semiconductors and insulators with a semilocal exchange-correlation potential, *Phys. Rev. Lett.* 102 (2009) 226401
 (b) J. Heyd, J.E. Peralta, G.E. Scuseria, R.L. Martin, Energy band gaps and lattice parameters evaluated with the Heyd-Scuseria-Ernzerhof screened hybrid functional, *J. Chem. Phys.* 123 (2005) 174101
 (c) J.P. Perdew, M. Levy, Physical content of the exact Kohn-Sham orbital energies: band gaps and derivative discontinuities, *Phys. Rev. Lett.* 51 (1983) 1884.
- [12] G.M. Rignanese, X. Rocquefelte, X. Gonze, A. Pasquarello, Titanium oxides and silicates as high-k dielectrics: a first-principles investigation, *Int. J. Quantum Chem.* 101 (2005) 793–801.
- [13] M.D. Segall, R. Shah, C.J. Pickard, M.C. Payne, Population analysis of plane-wave electronic structure calculations of bulk materials, *Phys. Rev. B* 54 (1996) 16317.
- [14] (a) Z.J. Wu, E.J. Zhao, H.P. Xiang, X.F. Hao, X.J. Liu, J. Meng, Crystal structures and elastic properties of superhard IrN₂ and IrN₃ from first principles, *Phys. Rev. B* 76 (2007) 054115
 (b) Q.J. Liu, Z. Ran, F.S. Liu, Z.T. Liu, Phase transitions and mechanical stability of TiO₂ polymorphs under high pressure, *J. Alloy. Compd.* 631 (2015) (192–054201).
- [15] N. Seriani, C. Pinilla, S. Scandolo, Titania–silica mixed oxides investigated with density functional theory and molecular dynamics simulations, *Phys. Status Solidi B* (2016). <http://dx.doi.org/10.1002/pssb.201600510>.
- [16] W. Voigt, *Lehrbuch der Kristallphysik*, Teubner, Leipzig, 1928.
- [17] A. Reuss, Calculation of the flow limits of mixed crystals on the basis of the plasticity of monocrystals, *Z. Angew. Math. Mech.* 9 (1929) 49.
- [18] R. Hill, The elastic behaviour of a crystalline aggregate, *Proc. Phys. Soc. Lond.* 65 (1952) 349.
- [19] S.F. Pugh, XCII. Relations between the elastic moduli and the plastic properties of polycrystalline pure metals, *Lond. Edinb. Dublin Philos. Mag. J. Sci.: Ser. 7* (45) (1954) 823–843.
- [20] S. Tian, *Materials Physical Properties*, Beijing, University of Aeronautics and Astronautics Press, Beijing, 2004.
- [21] (a) S.K. Saha, G. Dutta, Elastic and thermal properties of the layered thermoelectrics BiOCuSe and LaOCuSe, *Phys. Rev. B* 94 (2016) 125209
 (b) B. Salmankurt, S. Duman, First-principles study of structural, mechanical, lattice dynamical and thermal properties of nodal-line semimetals ZrXY (X=Si,Ge; Y=S,Se), *Philos. Mag.* (2016). <http://dx.doi.org/10.1080/14786435.2016.1250967>
 (c) P.J. Ying, X. Li, Y.C. Wang, J. Yang, C.G. Fu, W.Q. Zhang, X.B. Zhao, T.J. Zhu, Hierarchical chemical bonds contributing to the intrinsically low thermal conductivity in α -MgAgSb thermoelectric materials, *Adv. Funct. Mater.* (2016). <http://dx.doi.org/10.1002/adfm.201604145>.
- [22] (a) R. Vali, Band structure and dielectric properties of orthorhombic SrZrO₃, *Solid State Commun.* 145 (2008) 497–501
 (b) Y. Cai, L. Zhang, Q. Zeng, L. Cheng, Y. Xu, First-principles study of vibrational and dielectric properties of β -Si₃N₄, *Phys. Rev. B* 74 (2006) 174301
 (c) X. Gonze, C. Lee, Dynamical matrices, Born effective charges, dielectric permittivity tensors, and interatomic force constants from density-functional perturbation theory, *Phys. Rev. B* 55 (1997) 10355–10368.
- [23] X.C. Shen, *Semiconductor Spectroscopy and Optical Properties*, 2nd ed., Science Press, Beijing, 1992.
- [24] Q.J. Liu, Z.T. Liu, L.P. Feng, H. Tian, First-principles study of structural, elastic, electronic and optical properties of orthorhombic GaPO₄, *Solid State Sci.* 13 (2011) 1076–1082.